

SCIENTIFIC REPORTS



OPEN

A new fluorescent probe for colorimetric and ratiometric detection of sulfur dioxide derivatives in liver cancer cells

Received: 12 October 2016

Accepted: 23 February 2017

Published: 28 March 2017

Dong-Peng Li¹, Zhao-Yang Wang², Jie Cui¹, Xin Wang¹, Jun-Ying Miao² & Bao-Xiang Zhao¹

A new ratiometric fluorescent probe was constructed with hemicyanine and 7-nitrobenzofurazan for detection of sulfur dioxide derivatives ($\text{HSO}_3^-/\text{SO}_3^{2-}$). The ratiometric response mode could be attributed to the efficient FRET (Förster resonance energy transfer) platform. The probe exhibited some desirable properties including fast response (within 2 minutes), good selectivity and high sensitivity. Moreover, the probe could detect endogenous HSO_3^- in liver cancer cells rather than normal liver cells, implying the diagnosal potential of the probe.

Sulfur dioxide is one of the major origins of acid rain, putting serious impacts on water and soil¹. People who ever exposed to high levels of sulfur dioxide might suffer respiratory and cardiovascular diseases, lung cancer or neurological disorders². However, research revealed that sulfur dioxide could be produced in cytosols and mitochondria of cells³. The main raw materials for sulfur dioxide generation in cells are hydrogen sulfide (H_2S) and sulfur-containing amino acids³. On account of its functions in many physiological processes and physiopathology, sulfur dioxide was recognized as a new gaseous transmitter⁴. However, study of sulfur dioxide in living systems is still in its infancy. Lacking reliable analytical methods is one of the main bottlenecks.

Sulfur dioxide can easily dissolve in water (94 mg mL⁻¹, 25 °C) to form sulfite (SO_3^{2-}) and bisulfite (HSO_3^-) anions. So the physiological effects of sulfur dioxide can be attributed to its derivatives ($\text{HSO}_3^-/\text{SO}_3^{2-}$). Traditionally, many methods such as titrimetry, chromatography, electrochemistry and capillary electrophoresis are available for the detection of $\text{HSO}_3^-/\text{SO}_3^{2-}$ ^{5–8}. However, these methods usually suffered long operation time, low sensitivity, tedious operation and no applications inside living cells. Alternatively, fluorometric analysis has emerged in recent years, which could be used to detect analytes with high sensitivity and high accuracy^{9,10}. More importantly, *in situ* and real-time imaging of analytes could be carried out by non-destructive fluorescent probes^{11,12}.

Among fluorescent probes, ratiometric ones are more desirable than single intensity-based ones due to built-in correction of the two emission bands^{13,14}. By now, two detection mechanisms have been reported in the design of fluorescent probes for $\text{HSO}_3^-/\text{SO}_3^{2-}$: reactions with $\text{HSO}_3^-/\text{SO}_3^{2-}$ and hydrogen-bond formation with $\text{HSO}_3^-/\text{SO}_3^{2-}$ ^{15,16}. The reactions with $\text{HSO}_3^-/\text{SO}_3^{2-}$ include cleavage of levulinate group^{17,18}, nucleophilic addition to aldehyde group^{19,20} or “C=C” double bond^{21–31}. However, the probes based on hydrogen-bond formation were sensitive to environment; The probes based on cleavage of levulinate group took too long (usually 20–60 minutes) to detect $\text{HSO}_3^-/\text{SO}_3^{2-}$ in real time; The probes based on nucleophilic addition to aldehyde group could only function well under acidic conditions (usually pH = 5). So we concentrated on developing new favorable probes by using nucleophilic addition reaction with “C=C” double bond.

Here a new ratiometric fluorescent probe (HCy-NBD) was constructed by connecting hemicyanine and 7-nitrobenzofurazan with a piperazine moiety as the non-conjugate “bridge”. Both the good overlap of the two bands (fluorescence emission band of 7-nitrobenzofurazan fluorophore and absorption band of hemicyanine fluorophore) and the proper space distance between the two fluorophores benefit the FRET process in HCy-NBD. As a result, the 7-nitrobenzofurazan fluorophore may emit very weak fluorescence while the hemicyanine fluorophore may emit strong fluorescence. Upon nucleophilic addition of $\text{HSO}_3^-/\text{SO}_3^{2-}$ to the hemicyanine

¹Institute of Organic Chemistry, School of Chemistry and Chemical Engineering, Shandong University, Jinan 250100, P.R. China. ²Institute of Developmental Biology, School of Life Science, Shandong University, Jinan 250100, P.R. China. Correspondence and requests for materials should be addressed to B.-X.Z. (email: bxzhao@sdu.edu.cn)

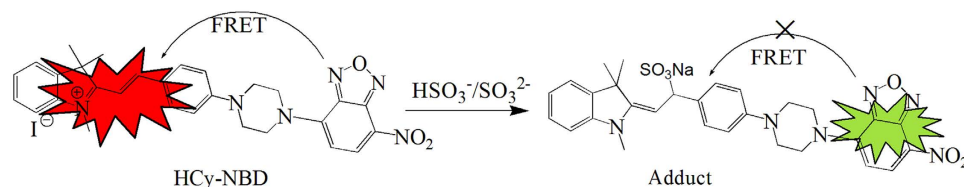


Figure 1. The structure of probe HCy-NBD and the proposed sensing mechanism.

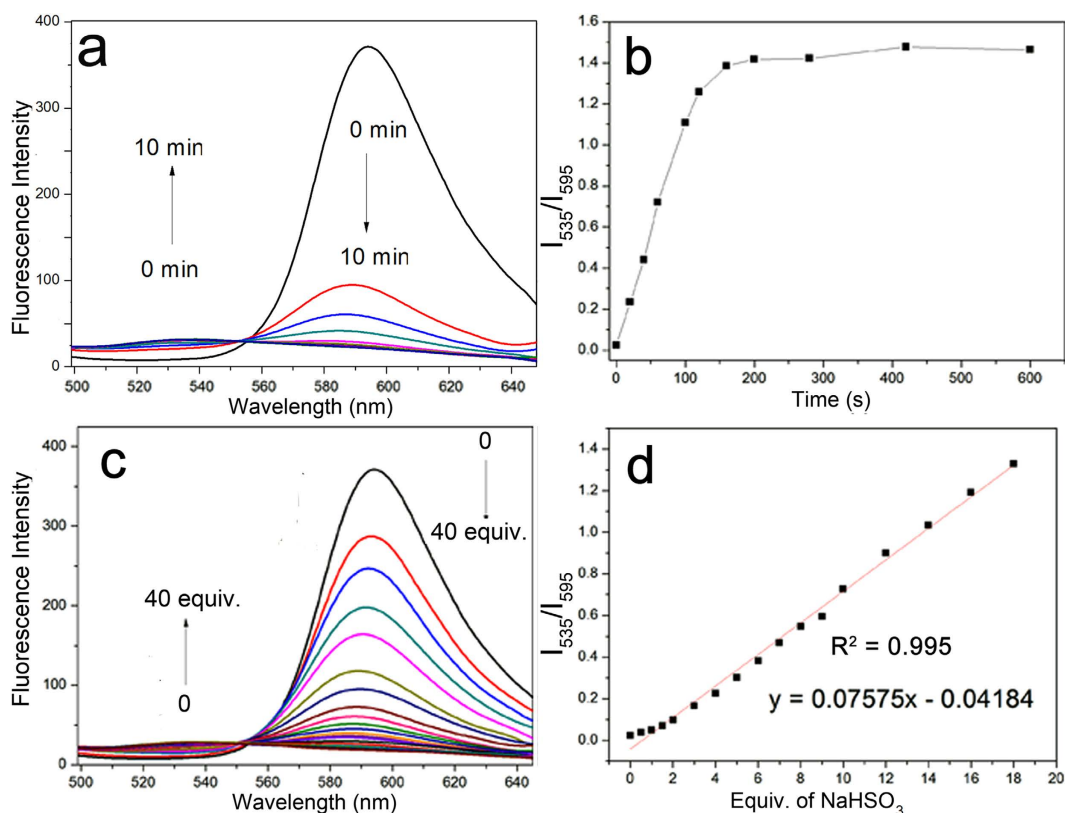


Figure 2. Fluorescence response of probe HCy-NBD toward NaHSO_3 . (a) and (b) Fluorescence changes of HCy-NBD in the presence of NaHSO_3 (25 equiv.) in 10 min. (c) Fluorescence titration spectra of HCy-NBD upon addition of NaHSO_3 (0–40 equiv.). (d) The linear relationship between I_{535}/I_{595} and NaHSO_3 (0–18 equiv.). $[\text{HCy-NBD}] = 10 \mu\text{M}$; Buffer: 50 mM Tris-HCl containing 40% ethanol; $\lambda_{\text{ex}} = 345 \text{ nm}$, slit: 10 nm/12 nm.

fluorophore, the conjugated system was broken and the FRET process was blocked, restoring the fluorescence of the 7-nitrobenzofurazan fluorophore. The proposed sensing mechanism was shown in Fig. 1.

Results and Discussion

Response of probe HCy-NBD toward bisulfite in aqueous solution. NaHSO_3 was used as donor of $\text{HSO}_3^-/\text{SO}_3^{2-}$. In the presence of 25 equiv. of NaHSO_3 , the emission band peaked at 595 nm decreased gradually, while a new band peaked at 535 nm gradually increased. The intensity ratios of the two emission bands (I_{535}/I_{595}) changed by a 61-fold from 0.024 to 1.47. The space between the two bands was much wider to avoid the overlap (Supplementary Table 1)³². The reaction could complete rapidly (in 2 min), which was suitable for real-time detection (Fig. 2, Supplementary Fig. 1). Upon addition of NaHSO_3 (0–40 equiv.) to the buffer solution of the probe, I_{535}/I_{595} changed quantitatively depending on NaHSO_3 concentrations (Fig. 2, Supplementary Fig. 2). A good linear relationship between I_{535}/I_{595} and the concentrations of NaHSO_3 (0–18 equiv.) was observed. Based on the linearity, the detection limit was determined to be 68 nM ($S/N = 3$), which was superior to many reported probes^{33–35}.

Among various anions and biothiols, only NaHSO_3 and Na_2SO_3 could lead to naked-eye changes in the colour of probe solutions (Supplementary Fig. 3). This implied the potential of probe HCy-NBD for colorimetric and selective detection of $\text{HSO}_3^-/\text{SO}_3^{2-}$. The good selectivity was further verified by fluorescence measurements (Fig. 3, Supplementary Fig. 4). Common biological relevant anions and small molecules including CN^- , HS^- and biothiols hardly brought about significant fluorescence changes. The good selectivity could be well understood

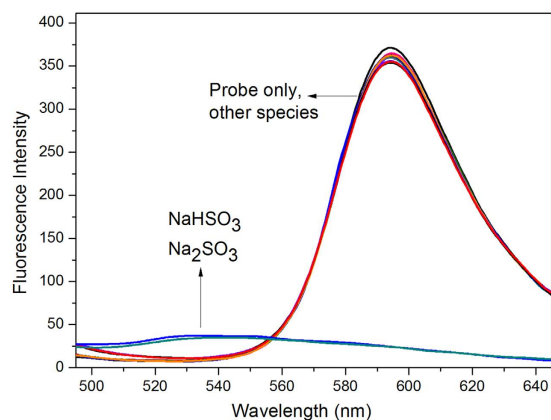


Figure 3. Fluorescence response of probe HCy-NBD toward various species. Species containing F^- , Cl^- , Br^- , I^- , HCO_3^- , NO_3^- , SO_4^{2-} , ClO^- , H_2O_2 , CN^- , SCN^- , $S_2O_3^{2-}$, HS^- , Cys, Hcy, GSH, HSO_3^- and SO_3^{2-} were involved. Final concentration for all the species was $250 \mu M$ except for Cys, Hcy and GSH (1 mM). $\lambda_{ex} = 345 \text{ nm}$, slit: $10 \text{ nm}/12 \text{ nm}$.

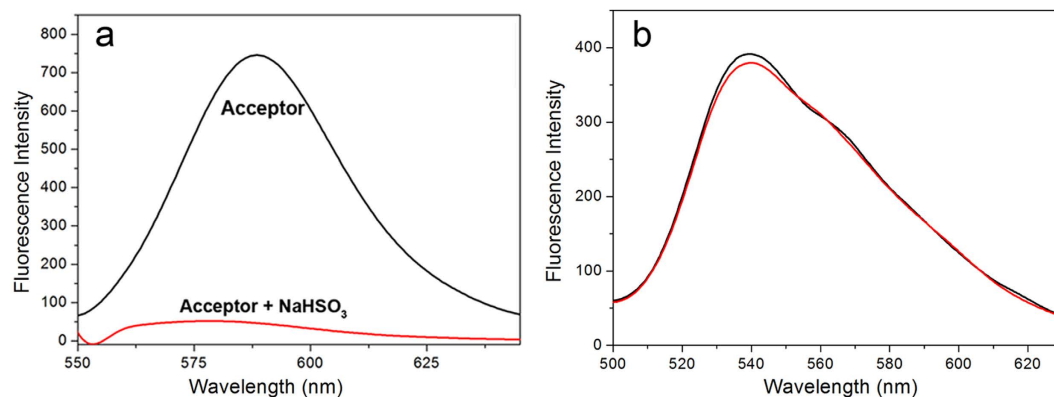


Figure 4. Fluorescence spectra of compound Acceptor and compound Donor in the presence of $NaHSO_3$. Fluorescence of compound Acceptor (a) and compound Donor (b) in the absence or presence of $NaHSO_3$. $NaHSO_3$ was 20 equiv. to that of Donor or Acceptor. $\lambda_{ex} = 345 \text{ nm}$ for the Donor and $\lambda_{ex} = 530 \text{ nm}$ for the Acceptor, slit: $10 \text{ nm}/12 \text{ nm}$.

by the strong nucleophilic ability of HSO_3^-/SO_3^{2-} under neutral conditions. It was reported that HS^- could react with 7-nitrobenzofurazan moiety to quench fluorescence³⁶. So compound Donor (Supplementary Scheme 1) was used to reveal the reactivity toward HS^- . Results showed that the fluorescence of compound Donor was almost unaffected, even with 100 equiv. HS^- for up to 1 h (Supplementary Fig. 5). The reactivity of probe HCy-NBD toward $NaHSO_3$ was almost unaffected in the presence of various species (Supplementary Fig. 6).

Mechanisms. The solution pH could usually put large impacts on the detection by affecting the state of reactants ($NaHSO_3$ and HCy-NBD) or the reaction efficiency between them³⁷. The fluorescence of probe HCy-NBD was almost constant in the range of pH 4–8. The stronger the basicity of the solution, the easier the reaction between probe HCy-NBD and $NaHSO_3$. (Supplementary Fig. 7). So it was the nucleophilicity of $NaHSO_3$ that was mainly affected by changing its existence forms³⁸.

Hemicyanine moiety is electrophilic and is liable to react with nucleophilic HSO_3^-/SO_3^{2-} . Upon addition of $NaHSO_3$, the fluorescence emission band of the Acceptor (Supplementary Scheme 1) diminished but that of the Donor was unaffected (Fig. 4). Furthermore, the UV-vis absorption spectra of probe HCy-NBD in the presence of $NaHSO_3$ ($0\text{--}300 \mu M$) were recorded (Fig. 5). The absorption band peaked at 530 nm which was assigned to hemicyanine moiety decreased and shifted to 490 nm which should belong to the absorption band of the 7-nitrobenzofurazan moiety (Fig. 5b). Meanwhile, a new band centred at 288 nm appeared. High-resolution mass spectroscopy revealed two dominant peaks at m/z 509.2304 and 591.2103, which could be ascribed to $[HCy-NBD + H]^+$ and $[HCy-NBD + HSO_3^-]^+$, respectively. (Supplementary Fig. 8). 1H NMR titration experiment also revealed the proposed reaction mechanism. The two peaks at about 8.3 and 7.3 ppm, which could be attributed to protons on the $C=C$ double bond of the probe, shifted to 4.8 and 4.9 ppm after reaction with Na_2SO_3 (Supplementary Scheme 2). Thus HSO_3^-/SO_3^{2-} was captured by the hemicyanine moiety via Michael addition reaction, which was in consistency with literatures^{27,39}.

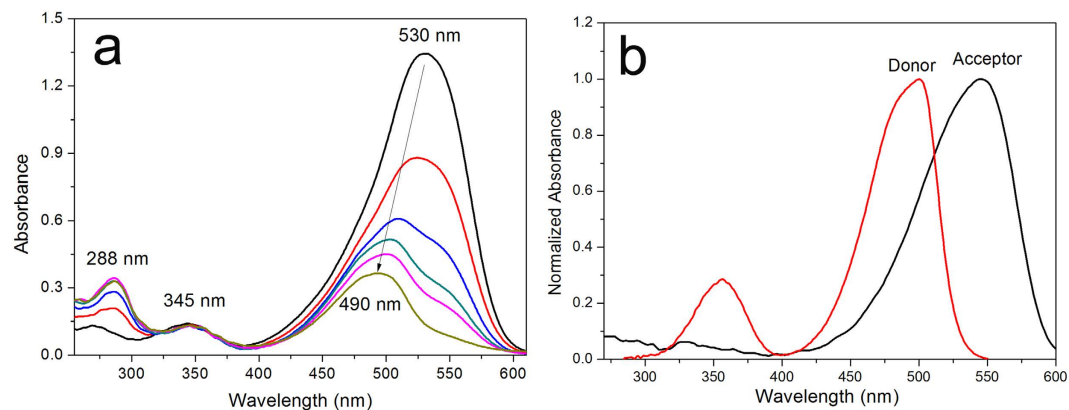


Figure 5. UV-vis spectra of HCy-NBD. (a) Absorption spectra of HCy-NBD (10 μM) in the presence of different amounts of NaHSO_3 (0–300 μM). (b) Normalized absorption spectra of compound Donor and Acceptor.

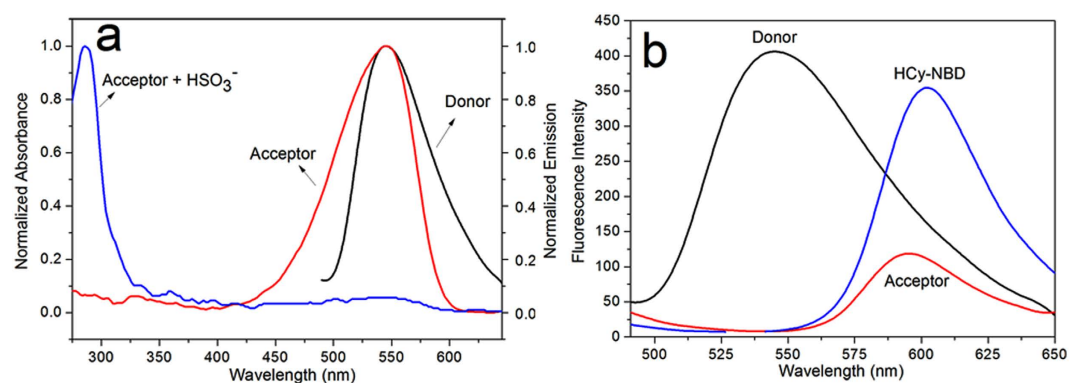


Figure 6. Interpretation of FRET process in HCy-NBD. (a) Normalized fluorescence spectrum of the Donor; Normalized UV-vis absorption spectrum of the Acceptor before and after addition of NaHSO_3 (20 equiv.). (b) Fluorescence spectra of the Donor, Acceptor and probe HCy-NBD. $\lambda_{\text{exc}} = 345 \text{ nm}$, slit: 10 nm/12 nm. $[\text{Donor}] = 5 \mu\text{M}$, $[\text{Acceptor}] = [\text{HCy-NBD}] = 10 \mu\text{M}$.

Absorption spectra of compound Acceptor overlapped greatly with the fluorescence spectra of compound Donor (Fig. 6a). Thus the fluorescence of the 7-nitrobenzofurazan moiety would be quenched because of the energy transfer to the hemicyanine moiety via FRET process^{40,41}. The FRET efficiency was determined to be 0.72. Interruption of the conjugated system in the hemicyanine moiety led to its absorption band blue-shifted greatly. So the abovementioned essential spectral overlap disappeared, and 7-nitrobenzofurazan moiety would emit fluorescence as a result. From the view of fluorescence intensity, the fluorescence of probe HCy-NBD was much greater than that of compound Acceptor excited at 345 nm, which further confirmed the FRET process in HCy-NBD (Fig. 6b).

Applications of probe HCy-NBD in living cells. Probe HCy-NBD showed excellent photostability in living cells (Supplementary Fig. 9) and ignorable cytotoxicity (Supplementary Fig. 10). Thus probe HCy-NBD could be suitable for $\text{HSO}_3^-/\text{SO}_3^{2-}$ detection in living cells with minimum interference. Exogenous HSO_3^- imaging experiments were primarily conducted in Hela cells. The ratios of fluorescence intensity ($I_{\text{green}}/I_{\text{red}}$) increased with the gradual increase of exogenous HSO_3^- (Supplementary Fig. 11). L-02 cells treated with NaHSO_3 (100 μM) and HCy-NBD (5 μM) showed 8-fold enhancement in the fluorescence intensity ratio compared with control group, which was much more sensitive than the previous reported probe HCy-D (Fig. 7)³².

Endogenous HSO_3^- could be produced with the help of TST enzyme⁴², which is widespread in nature and especially abundant in human liver cells⁴³. HepG2 cells and L-02 cells were separately incubated with HCy-NBD (5 μM) for 1 h, followed by incubation with GSH (500 μM) and $\text{Na}_2\text{S}_2\text{O}_3$ (250 μM) for another 0.5 h. Remarkable fluorescence change was observed only in HepG2 cells (Figs 7 and 8). By contrast, no significant fluorescence change was observed in HepG2 cells incubated with HCy-NBD and GSH. Moreover, HepG2 cells pre-treated with HCy-NBD (5 μM) and TNBS (10 mM, 2,4,6-trinitrobenzenesulphonate, known as a TST inhibitor) then with GSH (500 μM) and $\text{Na}_2\text{S}_2\text{O}_3$ (250 μM) showed no significant fluorescence change (Fig. 8). These results indicated that the endogenous HSO_3^- produced enzymatically in HepG2 cells was responsible for the fluorescence change.

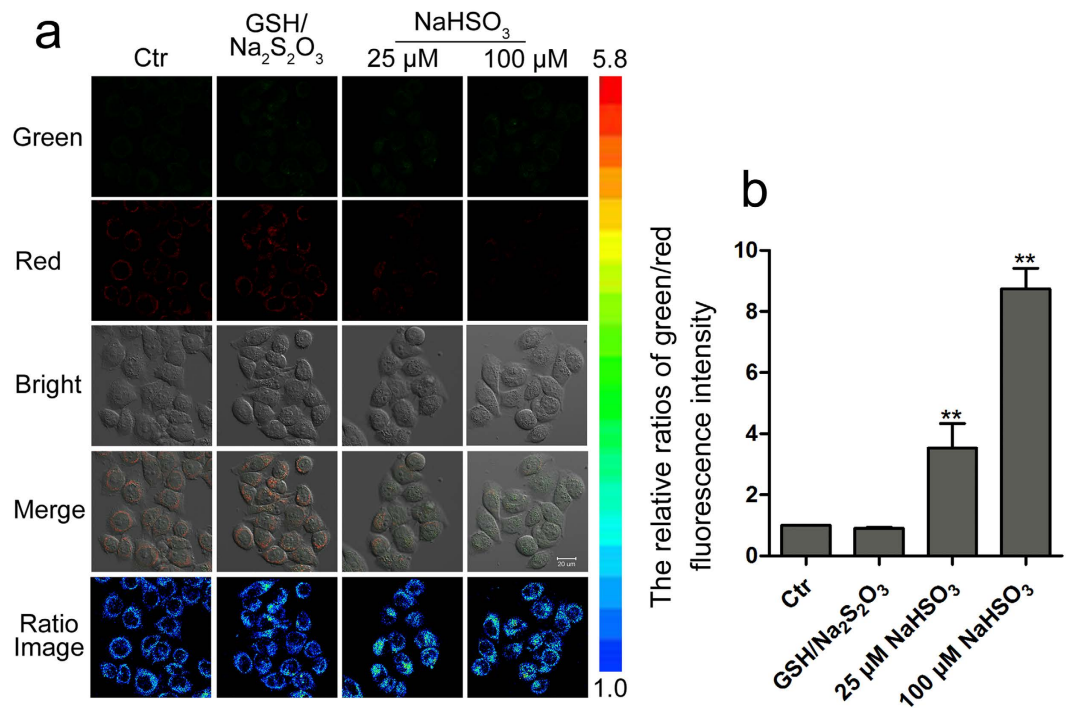


Figure 7. Detection of bisulfite in living L-02 cells. (a) Fluorescence, bright field and ratio images of L-02 cells which were incubated with HCy-NBD (5 μM) for 1 h, then with GSH (500 μM)/Na₂S₂O₃ (500 μM) or NaHSO₃ (25, 100 μM) for another 0.5 h. (b) The relative ratios of green/red fluorescence intensity. Images were acquired from 405–555 nm for green fluorescence, and from 560–700 nm for red fluorescence.

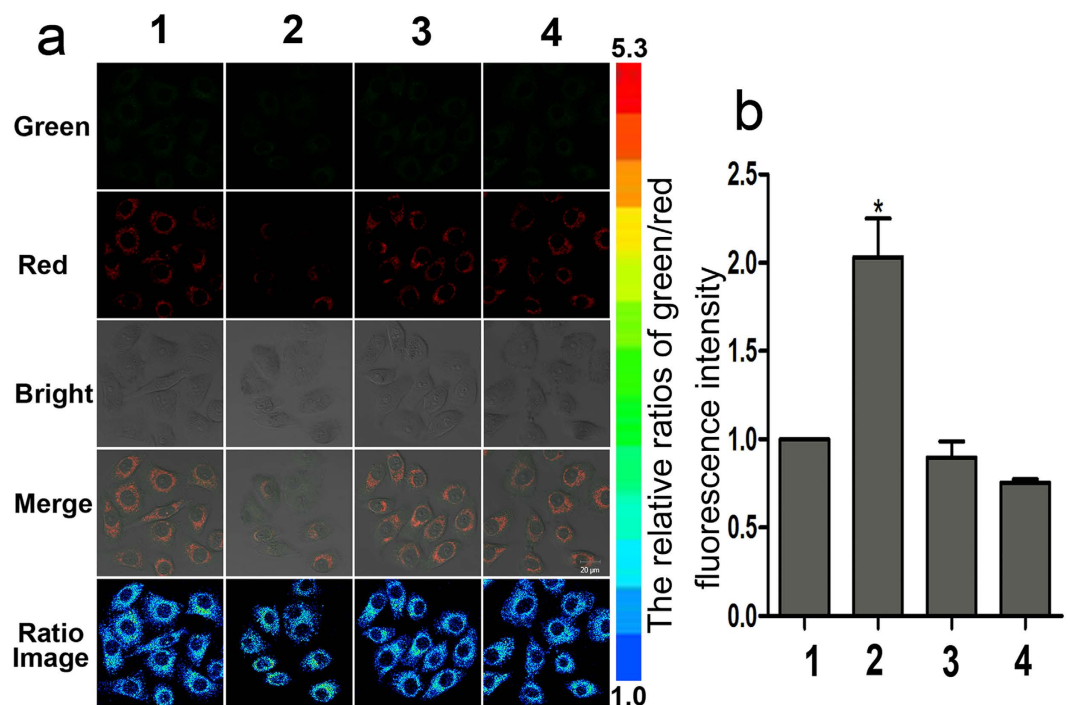


Figure 8. Detection of bisulfite in living HepG2 cells. (a) Row 1: HepG2 cells were incubated with HCy-NBD for 1 h; Row 2: HepG2 cells were incubated with HCy-NBD for 1 h, and then with GSH (500 μM) and Na₂S₂O₃ (250 μM) for 0.5 h; Row 3: HepG2 cells were incubated with HCy-NBD for 1 h, then with TNBS (10 mM) for 0.5 h, GSH (500 μM) and Na₂S₂O₃ (250 μM) for another 0.5 h; Row 4: HepG2 cells were incubated with HCy-NBD for 1 h, then with GSH (500 μM) for another 0.5 h. (b) The relative ratios of green/red fluorescence intensity of row 1, 2, 3 and 4 in (a). The ratio images were all obtained as $F_{\text{green}}/F_{\text{red}}$. Images were acquired from 405–555 nm for green fluorescence, and from 560–700 nm for red fluorescence, respectively. [HCy-NBD] 5 μM. $\lambda_{\text{ex}} = 405 \text{ nm}$.

On the whole, endogenous HSO_3^- in liver cancer cells rather than in normal liver cells could be detected, which revealed a new diagnostic feature of liver cancer cells. Therefore, the new way based on cellular level could be promising in liver cancer diagnosis and pathogenesis study of liver cancer.

Conclusions

A new fluorescent probe based on an FRET platform was reported. The probe could detect $\text{HSO}_3^-/\text{SO}_3^{2-}$ rapidly, sensitively and selectively. The probe also showed high energy transfer efficiency, good biocompatibility and high reactivity toward $\text{HSO}_3^-/\text{SO}_3^{2-}$. Endogenous bisulfite was successfully detected in liver cancer cells by the probe, which might pave a new way for liver cancer diagnosis and pathogenesis study of liver cancer.

Methods

Apparatus and chemicals. ^1H NMR (300 or 400 MHz) and ^{13}C NMR (100 MHz) spectra were recorded on a Bruker Avance 300 or 400 spectrometer using CDCl_3 , $\text{DMSO}-d_6$ or D_2O as solvent and tetramethylsilane (TMS) as an internal standard. HR-MS spectra were recorded on a Q-TOF6510 spectrograph (Agilent). IR spectra were recorded by use of the IR spectrophotometer VERTEX 70 FT-IR (Bruker Optics). Melting points were measured on an XD-4 digital micro-melting point apparatus. Thin-layer chromatography (TLC) was conducted on silica gel 60F₂₅₄ plates (Merck KGaA) and column chromatography was conducted over silica gel (mesh 200–300). Fluorescence measurements were conducted on a Perkin-Elmer LS-55 luminescence spectrophotometer, and UV-vis spectra were recorded on a U-4100 UV-Vis-NIR Spectrometer (Hitachi). Quartz cuvettes with a 1 cm path length and 3-mL volume were involved in fluorescence and UV-vis absorption measurements. The pH values were measured by use of a PHS-3C digital pH-meter (YouKe, Shanghai). All reagents were purchased from J&K, Aladdin and Sinopharm Chemical Reagent Co. and used without further purification.

Preparation for UV-vis absorption and fluorescence spectral measurements. Tris-HCl buffer (50 mM, pH 7.4) was used throughout. HCy-NBD was dissolved in DMSO to get the stock solution (1 mM). Distilled water was used to prepare stock solutions (1 mM) of NaF, NaCl, NaBr, KI, NaHCO_3 , KNO_3 , NaClO, Na_2SO_4 , KSCN, $\text{Na}_2\text{S}_2\text{O}_3$, NaHS, Na_2SO_3 , NaHSO_3 , (n-Bu)₄CN, cysteine, homocysteine and glutathione. Stock solutions of NaHSO_3 and Na_2SO_3 were freshly prepared each time before use. Test solutions were prepared by placing the stock solution of HCy-NBD (100 μL) and an appropriate aliquot of each testing species solution into a 10-mL volumetric flask, and the solution was diluted to 10 mL with Tris-HCl buffer (50 mM, pH 7.4) containing 40% ethanol (v/v).

Cell imaging. L-02 cells or HepG2 cells were cultured in a 6-well plate in Dulbecco's modified Eagle's medium (DMEM) supplemented with 10% fetal bovine serum in an atmosphere of 5% CO_2 and 95% air at 37 °C. HCy-NBD was dissolved in DMSO to get the stock solution (10 mM) and diluted to 5 μM each time before use. L-02 cells or HepG2 cells were incubated with HCy-NBD (5 μM) for 1 h, then treated with exogenous substances. Subsequently, the cell images were taken under a confocal microscope (LSM 700) at emission channels of 405–555 nm (green channel) and 560–700 nm (red channel), respectively.

Synthesis and characterization of probe HCy-NBD. To ethanol (10 mL) was added compound 3 (320 mg, 0.67 mmol) and compound 4 (140 mg, 0.70 mmol) at room temperature (Supplementary Scheme 1). Then the mixture was stirred at room temperature for 5 h. The solvent was removed under reduced pressure, then the residue was subjected to column chromatography on silica gel (CH_2Cl_2 : MeOH = 10:1 to 1:1) to afford a dark red powder (390 mg, 91.0%). mp: >300 °C. ^1H NMR ($\text{DMSO}-d_6$, 400 MHz) δ (ppm): 8.55 (d, J = 9.2 Hz, 1H), 8.34 (d, J = 16 Hz, 1H), 8.14 (d, J = 8.8 Hz, 2H), 7.81–7.74 (m, 2H), 7.59–7.50 (m, 2H), 7.36 (d, J = 16 Hz, 1H), 7.08 (d, J = 8.8 Hz, 2H), 6.62 (d, J = 9.2 Hz, 1H), 4.39 (br, 4H), 4.02 (s, 3H), 3.96–3.93 (m, 4H), 1.77 (s, 6H); ^{13}C NMR ($\text{DMSO}-d_6$, 100 MHz) δ (ppm): 180.69, 154.30, 153.88, 145.95, 145.30, 143.26, 142.49, 136.79, 134.26, 129.22, 128.43, 124.00, 123.12, 121.58, 114.40, 13.26, 107.04, 103.27, 93.34, 51.63, 48.62, 44.98, 33.84; IR (KBr) cm^{-1} : 3082, 3037, 2970, 2923, 2856, 1574, 1525, 1479, 1373, 1291, 1189, 1171, 1112, 1015, 995, 929. HRMS: m/z calculated for $\text{C}_{29}\text{H}_{29}\text{N}_6\text{O}_3^+$: 509.2301, found: 509.2300.

References

1. Streets, D. G., Carmichael, G. R. & Arndt, R. L. Sulfur dioxide emissions and sulfur deposition from international shipping in Asian waters. *Atmos. Environ.* **31**, 1573–1582 (1997).
2. Claudia, R. C. & Francisco J. C. Application of flow injection analysis for determining sulphites in food and beverages: A review. *Food Chem.* **112**, 487–493 (2009).
3. Griffith, O. W. Cysteine sulfinate metabolism altered partitioning between transamination and decarboxylation following administration of β -methyleneaspartate. *J. Biol. Chem.* **258**, 1591–1598 (1983).
4. Meng, Z., Yang, Z., Li, J. & Zhang, Q. The vasorelaxant effect and its mechanisms of sodium bisulfite as a sulfur dioxide donor. *Chemosphere* **89**, 579–584 (2012).
5. Lowinson, D. & Bertotti, M. Determination of sulphite in wine by colorimetric titration. *Food Addit. Contam.* **18**, 773–777 (2001).
6. Miura, Y., Hatakeyama, M., Hosino, T. & Haddad, P. R. Rapid ion chromatography of L-ascorbic acid, nitrite, sulfite, oxalate, iodide and thiosulfate by isocratic elution utilizing a postcolumn reaction with cerium(IV) and fluorescence detection. *J. Chromatogr. A* **956**, 77–84 (2002).
7. Yilmaz, Ü. T. & Somer, G. Determination of trace sulfite by direct and indirect methods using differential pulse polarography. *Anal. Chim. Acta* **603**, 30–35 (2007).
8. Palenzuela, B., Simonet, B. M., Ríos, A. & Valcárcel, M. Determination of free and total sulphur dioxide in wine by use of an amalgamated piezoelectric sensor. *Anal. Chim. Acta* **535**, 65–72 (2005).
9. Niu, W. *et al.* Highly selective two-photon fluorescent probe for ratiometric sensing and imaging cysteine in mitochondria. *Anal. Chem.* **88**, 1908–1914 (2016).
10. Yu, T. *et al.* A reversible and highly selective fluorescence “on-off-on” probe for detecting nickel ion in the mitochondria of living cells. *Biosen. Bioelectron.* **82**, 93–98 (2016).

11. Zhang, L. *et al.* A highly selective and sensitive near-infrared fluorescent probe for imaging of hydrogen sulphide in living cells and mice. *Sci. Rep.* **6**, 18868 (2016).
12. Zhang, N. *et al.* A novel fluorescent probe based on the flexible dipicolylamine: Recognizing zinc(II) in aqueous solution and imaging in living cell. *Dyes Pigm.* **124**, 174–179 (2016).
13. Liu, Y. *et al.* Rapid and ratiometric fluorescent detection of cysteine with high selectivity and sensitivity by a simple and readily available probe. *ACS Appl. Mater. Interfaces* **6**, 17543–17550 (2014).
14. Jiang, N. *et al.* Ratiometric fluorescence imaging of cellular polarity: decrease in mitochondrial polarity in cancer cells. *Angew. Chem. Int. Ed.* **54**, 2510–2514 (2015).
15. Sun, Y., Zhong, C., Gong, R., Mu, H. & Fu, E. A ratiometric fluorescent chemodosimeter with selective recognition for sulfite in aqueous solution. *J. Org. Chem.* **74**, 7943–7946 (2009).
16. Wang, C. *et al.* A new fluorescent turn-on probe for highly sensitive and selective detection of sulfite and bisulfite. *Sens. Actuators B* **190**, 792–799 (2014).
17. Choi, M. G., Hwang, J., Eor, S. & Chang, S. K. Chromogenic and fluorogenic signaling of sulfite by selective deprotection of resorufin levulinate. *Org. Lett.* **12**, 5624–5627 (2010).
18. Zhang, H., Xue, S. & Feng, G. A colorimetric and near-infrared fluorescent turn-on probe for rapid detection of sulphite. *Sens. Actuators B* **231**, 752–758 (2016).
19. Yang, X. F., Zhao, M. & Wang, G. A rhodamine-based fluorescent probe selective for bisulfite anion in aqueous ethanol media. *Sens. Actuators B* **152**, 8–13 (2011).
20. Liu, X. *et al.* A ratiometric fluorescent probe for rapid, sensitive and selective detection of sulfur dioxide with large Stokes shifts by single wavelength excitation. *Org. Biomol. Chem.* **13**, 8663–8668 (2015).
21. Zhang, H., Huang, Z. & Feng, G. Colorimetric and ratiometric fluorescent detection of bisulfite by a new HBT-hemicyanine hybrid. *Anal. Chim. Acta* **920**, 72–79 (2016).
22. Sun, Y. Q., Liu, J., Zhang, J., Yang, T. & Guo, W. Fluorescent probe for biological gas SO₂ derivatives bisulfite and sulphite. *Chem. Commun.* **49**, 2637–2639 (2013).
23. Tan, L., Lin, W., Zhu, S., Yuan, L. & Zheng, K. A coumarin-quinolinium-based fluorescent probe for ratiometric sensing of sulfite in living cells. *Org. Biomol. Chem.* **13**, 4637–4643 (2014).
24. Li, H. *et al.* A fluorescent probe for ratiometric imaging of SO₂ derivatives in mitochondria of living cells. *Ind. Eng. Chem. Res.* **55**, 1477–1483 (2016).
25. Peng, M. J. *et al.* A hybrid coumarin–thiazole fluorescent sensor for selective detection of bisulfite anions *in vivo* and in real samples. *Chem. Asian J.* **9**, 1817–1822 (2014).
26. Xu, W. *et al.* A mitochondria-targeted ratiometric fluorescent probe to monitor endogenously generated sulfur dioxide derivatives in living cells. *Biomaterials* **56**, 1–9 (2015).
27. Zhang, Q., Zhang, Y., Ding, S., Zhang, H. & Feng, G. A near-infrared fluorescent probe for rapid, colorimetric and ratiometric detection of bisulfite in food, serum, and living cells. *Sens. Actuators B* **211**, 377–384 (2015).
28. Wu, M. Y., Li, K., Li, C. Y., Hou, J. T. & Yu, X. Q. A water-soluble near-infrared probe for colorimetric and ratiometric sensing of SO₂ derivatives in living cells. *Chem. Commun.* **50**, 183–185 (2014).
29. Wu, W.-L. *et al.* An effective colorimetric and ratiometric fluorescent probe based FRET with a large Stokes shift for bisulfite. *Sci. Rep.* **6**, 25315 (2016).
30. Chen, W. *et al.* Selective, highly sensitive fluorescent probe for the detection of sulfur dioxide derivatives in aqueous and biological environments. *Anal. Chem.* **87**, 609–616 (2015).
31. Geng, L., Yang, X. F., Zhong, Y., Li, Z. & Li, H. “Quinone-phenol” transduction activated excited-state intramolecular proton transfer: A new strategy toward ratiometric fluorescent probe for sulfite in living cells. *Dyes Pigm.* **120**, 213–219 (2015).
32. Li, D. P. *et al.* A mitochondria-targeted fluorescent probe for ratiometric detection of endogenous sulfur dioxide derivatives in cancer cells. *Chem. Commun.* **52**, 2760–2763 (2016).
33. Wang, X. B. *et al.* Effect of sulfur dioxide preconditioning on rat myocardial ischemia/reperfusion injury by inducing endoplasmic reticulum stress. *Basic Res. Cardiol.* **106**, 865–878 (2011).
34. Ji, A. J., Savon, S. R. & Jacobsen, D. W. Determination of total serum sulfite by HPLC with fluorescence detection. *Clin. Chem.* **41**, 897–903 (1995).
35. Xu, J. *et al.* A mitochondria-targeted ratiometric fluorescent probe for rapid, sensitive and specific detection of biological SO₂ derivatives in living cells. *Biosens. Bioelectron.* **77**, 725–732 (2016).
36. Pak, Y. L. *et al.* Mitochondria-targeted reaction-based fluorescent probe for hydrogen sulfide. *Anal. Chem.* **88**, 5476–5481 (2016).
37. Niu, W. *et al.* Ratiometric emission fluorescent pH probe for imaging of living cells in extreme acidity. *Anal. Chem.* **87**, 2788–2793 (2015).
38. Yu, C., Luo, M., Zeng, F. & Wu, S. A fast-responding fluorescent turn-on sensor for sensitive and selective detection of sulfite anions. *Anal. Methods* **4**, 2638–2640 (2012).
39. Liu, Y. *et al.* A mitochondria-targeted colorimetric and ratiometric fluorescent probe for biological SO₂ derivatives in living cells. *Chem. Commun.* **51**, 10236–10239 (2015).
40. Wei, L. *et al.* FRET ratiometric probes reveal the chiral-sensitive cysteine-dependent H₂S production and regulation in living cells. *Sci. Rep.* **4**, 4521 (2014).
41. Fan, J., Hu, M., Zhan, P. & Peng, X. Energy transfer cassettes based on organic fluorophores: construction and applications in ratiometric sensing. *Chem. Soc. Rev.* **42**, 29–43 (2013).
42. Li, G. *et al.* A dinuclear iridium(III) complex as a visual specific phosphorescent probe for endogenous sulphite and bisulphite in living cells. *Chem. Sci.* **4**, 4426–4433 (2013).
43. Ploegman, J. H. *et al.* The covalent and tertiary structure of bovine liver rhodanase. *Nature* **273**, 124–129 (1978).

Acknowledgements

This study was supported by the Natural Science Foundation of Shandong Province (ZR2014BM004), Project of Science and Technology of Shandong Province (2016GSF121021), Major Project of Science and Technology of Shandong Province (2015ZDJS04001 and 2015ZDJS04003).

Author Contributions

B.-X.Z. designed the probe and revised the paper writing. J.-Y.M. guided the cell assays. D.-P.L. performed the probe synthesis, *in vitro* tests and paper writing. Z.-Y.W. performed the cell assays. J.C. and X.W. assisted the synthesis. All authors reviewed the manuscript.

Additional Information

Supplementary information accompanies this paper at <http://www.nature.com/srep>

Competing Interests: The authors declare no competing financial interests.

How to cite this article: Li, D.-P. *et al.* A new fluorescent probe for colorimetric and ratiometric detection of sulfur dioxide derivatives in liver cancer cells. *Sci. Rep.* **7**, 45294; doi: 10.1038/srep45294 (2017).

Publisher's note: Springer Nature remains neutral with regard to jurisdictional claims in published maps and institutional affiliations.



This work is licensed under a Creative Commons Attribution 4.0 International License. The images or other third party material in this article are included in the article's Creative Commons license, unless indicated otherwise in the credit line; if the material is not included under the Creative Commons license, users will need to obtain permission from the license holder to reproduce the material. To view a copy of this license, visit <http://creativecommons.org/licenses/by/4.0/>

© The Author(s) 2017